Ensemble Temperature and Precipitation Projection for Multi-Factorial Interactive Effects of GCMs and SSPs: Application to China

Ruixin Duan[1,2], Guohe Huang[1]*, Yongping Li[1], Rubing Zheng[2], Guoqing Wang[3], Baozhen Xin[3], Chuyin Tian[1,2] and Jiayan Ren[1,2]

[1]State Key Joint Laboratory of Environmental Simulation and Pollution Control, China-Canada Center for Energy, Environment and Ecology Research, UR-BNU, School of Environment, Beijing Normal University, Beijing, China, [2]Sino-Canada Resources and Environmental Research Academy, North China Electric Power University, Beijing, China, [3]State Key Laboratory of Hydrology–Water Resources and Hydraulic Engineering, Nanjing Hydraulic Research Institute, Nanjing, China

Climate change has broadly impacted on the China areas. There will be severe challenges due to the variations of precipitation and temperature in the future. Therefore, a comprehensive understanding of the future climate change over China areas is desired. In this study, future annual precipitation and annual mean temperature under two SSPs over China areas were projected through multiple global climate models. Meanwhile, to explore the sources of uncertainty in projecting future climate change, the multi-factorial analysis was conducted through GCMs (five levels) and SSPs (two levels). This study can help us understand the possible changes in precipitation, temperature, and the potential extreme climate events over the China area. The results indicate that China would have more annual precipitation and higher annual mean temperature in the future. Compared with the historical period, the annual mean temperature would face a continuously increasing trend under SSPs. Regardless of SSP245 or SSP585, the growth rate of annual precipitation and annual mean temperature increase in the northern region (e.g., Northeast China, North China, and Northwest China) are higher than those in the southern parts (e.g., East China, South China, and Central China). The future temperature rise may increase the frequency of heat-related extreme climate events, which needs to be focused on in future research. Moreover, GCM was the main contributing factor to the sources of uncertainty in projecting future precipitation and SSP was the main factor for future temperature. Overall, climate change is an indisputable fact in China. The annual precipitation and annual mean temperature would increase to varying degrees in the future. Reducing the systemic bias of the climate model itself will undoubtedly be the top priority, and it would help to improve the projection and evaluation effects of relevant climate variables.

Keywords: climate change, annual precipitation, annual mean temperature, multi-factorial analysis, China

INTRODUCTION

Temperature and precipitation are the two major climatic elements that people are most concerned about under climate change (Tisseuil et al., 2012). Observations show that the average temperature of the global land area has been increasing significantly, especially in recent decades (Cheng et al., 2019). Not only that, but the precipitation has also changed to varying degrees. Changes in temperature and precipitation will cause a series of extreme climate events (Kodinariya and Makwana, 2013; Duan et al., 2020). For instance, droughts and heatwaves have increased, and floods have become more frequent (Wang et al., 2004b). There is no doubt that the intensification of climate change has affected the survival and development of humans (Feng and Hu, 2014). Besides, changes in precipitation and temperature also affect agricultural, industrial, fisheries, animal husbandry, and other aspects. Therefore, the assessment of future temperature and precipitation will help to improve the ability to deal with climate-related impacts (Wang et al., 2018). Precipitation and temperature in China have also seen significant changes in recent decades (Shivam et al., 2019). The increase in climate disasters caused by climate warming may be a more prominent problem in China. This may bring frequent climatic disasters, including excessive rainfall, extensive droughts, and sustained high temperatures, resulting in large-scale disaster losses. Therefore, the projection and analysis of future climate change have important socio-economic significance (Ghosh and Mujumdar, 2007; Zhai et al., 2020).

Previous studies have checked future changes in temperature and precipitation in China by multiple climate models (e.g., global climate models and regional climate models) (Du et al., 2018; Jacob et al., 2018). Most research focused on analyzing the temporal and spatial characteristics of key climate elements. Besides, the quantitative analysis of climate elements was also one of the current research hotspots. In particular, the changes in relative historical periods such as temperature and precipitation under different emission scenarios in the future (Cho et al., 2015; Ji et al., 2018; Batibeniz et al., 2020). There is no doubt that the climate model has become an important tool for assessing future climate change in the current period. For example Hui et al. (2018), analyzed the mean and extreme climate over China during future period through the simulations from global climate models (GCMs) under two RCPs (Representative Concentration Pathways). Ultimately, the study revealed that China area would experience much warmer climate in the future (Hui et al., 2018). Ba et al. (2018) assessed the impacts of climate change on water resources in Kaidu River Basin through multiple general circulation models under two RCPs. The results showed that both the precipitation and temperature in the study area would increase in the future relative to the historical period (Ba et al., 2018). Hou et al. (2019) compared the performance of multiple climate models for future climate change projection over different regions in China (Hou et al., 2019).

However, many studies were mainly focused on analyzing the future changes in precipitation and temperature through individual global climate models (GCMs) from CMIP5

(Manrique-Alba et al., 2020). Currently, the GCMs are the only tool available to project future climate change. They have been widely used in assessing climate change (Thomas et al., 2013). Due to the lack of a full understanding of the complex climate change process, there are inevitably many deficiencies in GCMs (Paeth and Hense, 2004; Dan et al., 2015; Spinoni et al., 2019). The grid points of GCMs are often larger than 100 km, which makes them difficult to employ for regional climate change research. Besides, due to the uncertainty of emission scenarios, climate change in the future is often uncertain (Carrão et al., 2016; Park et al., 2016; Peltier et al., 2018). Although existing studies have analyzed the uncertainties of climate models and emission scenarios for future climate projections, they have seldom considered their interactive effects (Vogel et al., 2020). Moreover, the new version of climate models has improved the ability to simulate climate elements. Therefore, it is necessary to strengthen the analysis of future climate change under the latest coupled model. (i.e., CMIP6).

Therefore, as an extension of previous studies, the objective of this research is to evaluate the possible changes in annual precipitation and annual mean temperature in China and trace the sources of uncertainty on projecting future climate change. Specifically, the objective entails 1) exploring changes in temperature and precipitation in the future from multiple perspectives through an ensemble of multiple GCMs under different Shared Socioeconomic Pathways (SSPs), 2) quantifying the main contribution (and their interactions) of climate models and emission scenarios to the sources of uncertainty on climate change projection.

METHODOLOGY AND CLIMATE DATA

Study Area

The terrain of China is high in the west and low in the east and is complex and diverse (Smirnov et al., 2016; Poschlod et al., 2018; Zhou et al., 2018). Mountains accounted for 33.3% of the total land area, plateaus accounted for 26%, basins accounted for 18.8%, plains accounted for 12%, and hills accounted for 9.9% (Sharafi et al., 2020). The terrain forms a three-level ladder from west to east. Among them, the Qinghai-Tibet Plateau is located in the west, with the highest terrain. It is composed of extremely high mountains and plateaus. Therefore, it is also called the "roof of the world". The second ladder is from the east of the Qinghai-Tibet Plateau to Daxinganling-Taihang-Wushan-Xuefeng Mountain (Tan et al., 2011; Thompson et al., 2016). The altitude is generally 1,000–2000 m, and it is mainly composed of mountains, plateaus, and basins. The broad plains and hills of eastern China are the third ladder. The annual precipitation gradually decreases from the southeast coast to the northwest inland. The annual precipitation in the southeast coastal area is more than 1,600 mm and decreases to 800 mm near the Qinling-Huaihe River. Then to the northwest to Daxinganling-Yinshan-Lanzhou-southeast of the Qinghai-Tibet Plateau, it is reduced to 400 mm. The Helan Mountain to the central part of the Qinghai-Tibet Plateau reduces to 200 mm. The annual precipitation in the Tarim Basin is less than 50 mm (Moore et al., 2013). The
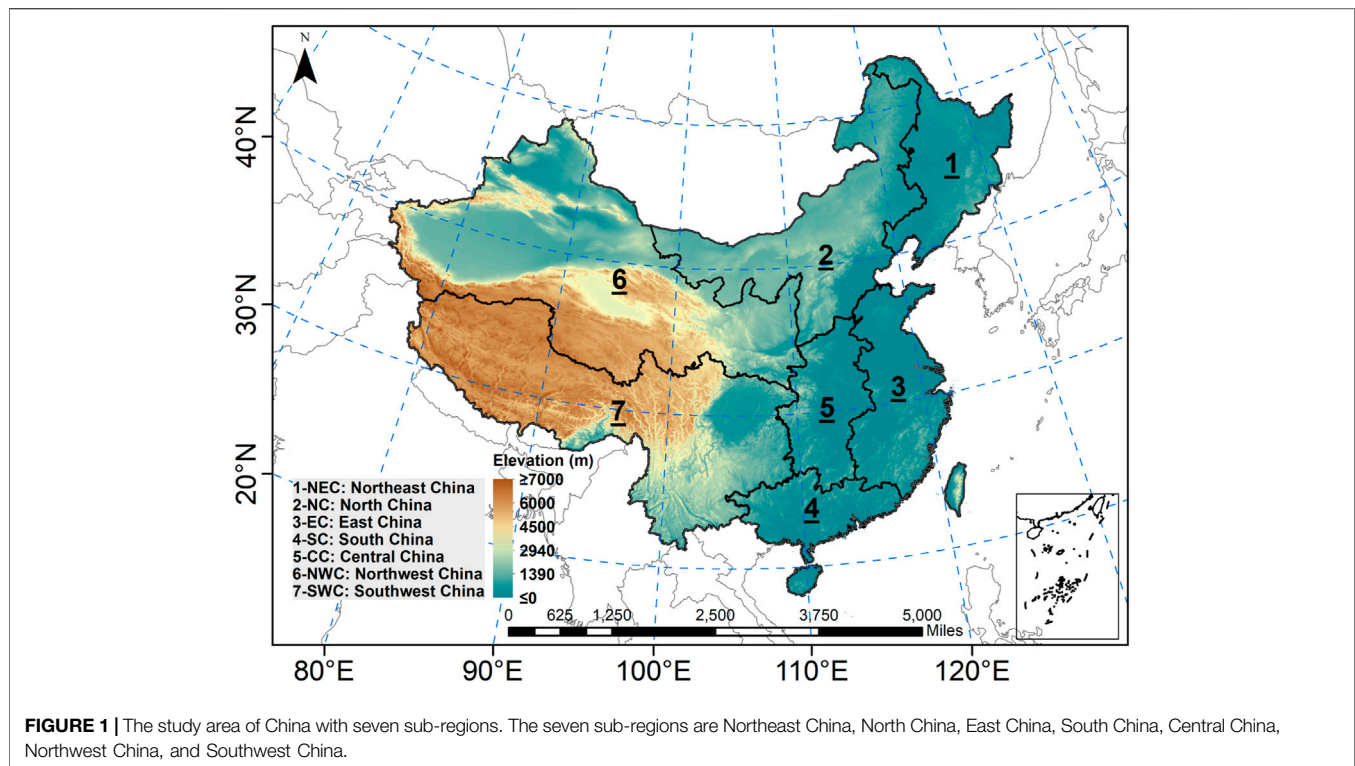
FIGURE 1 | The study area of China with seven sub-regions. The seven sub-regions are Northeast China, North China, East China, South China, Central China, Northwest China, and Southwest China.

TABLE 1 | The information of five global climate models employed in this study.

GCM model	Resolution (deg)	Experiment	Time frequency	Variant Label
CESM2	1.25 × 0.94	historical, ssp245, ssp585	Mon	r1i1p1f1
GFDL-ESM4	1.25 × 1.0	historical, ssp245, ssp585	Mon	r1i1p1f1
IPSL-CM6A-LR	2.50 × 1.27	historical, ssp245, ssp585	Mon	r1i1p1f1
MIROC6	1.41 × 1.40	historical, ssp245, ssp585	Mon	r1i1p1f1
MRI-ESM2-0	1.125 × 1.12	historical, ssp245, ssp585	Mon	r1i1p1f1

temperature difference between north and south is large in winter, while the south is warm, and the temperature gets lower as it goes north. The summer is generally high throughout the country, and the Qinghai-Tibet Plateau is the coolest place in China. Due to the combined influence of human activities and natural factors, the annual average temperature in China has risen by 0.68°C since the 1950s. Therefore, it is imminent to carry out climate change projection and assessment over China. The changes in precipitation and temperature in different regions of China are not the same. To facilitate comparative analysis, China is divided into seven subregions, including Northeast China, North China, East China, South China, Central China, Northwest China, and Southwest China, as shown in **Figure 1**. The division of subregions refers to previous studies (Smalley et al., 2019).

Dataset

Five different kinds of GCMs (i.e., CESM2, GFDL-ESM4, IPSL-CM6A-LR, MIROC6, and MRI-ESM2-0) are acquired from the WCRP Coupled Model Intercomparison Project (Phase 6)

dataset archive (https://esgf-node.llnl.gov/projects/cmip6/). The details are shown in **Table 1**. Two 50-year periods are employed in this study, including the historical period (1965–2014) and the future period (2051–2100). The data in the future period is extracted under two SSPs (i.e., SSP245 and SSP585). The annual precipitation and annual mean temperature are the two variables of interest in this study. The data are all united to 0.5° × 0.5° in spatial through the bilinear interpolation method (Chen et al., 2016). The SSPs (Shared Socioeconomic Pathways) is the latest scenarios to project socioeconomic global changes up to 2100. They are broadly employed to derive greenhouse gas emissions scenarios with different climate policies. The SSP245 scenario assumes that the world follows a path where social, economic, and technological trends will not significantly deviate from historical patterns. Among them, development and income growth are not balanced. Some countries have made good progress, while others have fallen short of expectations. The environmental system has experienced degradation, but there have been some improvements, and the intensity of resource and energy use has declined overall (Ying et al., 2019). Global

population growth is modest and stabilized in the second half of this century. Income inequality persists or is slow to improve, and the challenge of reducing vulnerability to social and environmental changes remains (Roberts et al., 2019; Asif and Chen, 2020; Li et al., 2020). SSP585 assumes that the world increasingly believes that competitive markets, innovation, and a participatory society can bring rapid technological progress and human capital development as a way to sustainable development. At the same time, while promoting economic and social development, all parts of the world are developing abundant fossil fuel resources and adopting resource- and energy-intensive lifestyles. All these factors have led to the rapid growth of the global economy, while the global population has reached its peak and declined in the 21st century (Trenberth and Shea, 2005).

Multi-Factorial Analysis Method

The main content of the multi-factorial analysis method is the Analysis of variance (ANOVA) theory (Li et al., 2010). As an effective statistical method, the main contribution and the interactions of multiple factors to the sources of uncertainty can be traced. In this study, the global climate models (i.e., GCMs) and emission scenarios (i.e., SSPs) are the two sources of uncertainty on future precipitation and temperature projection. It has been broadly used to address the non-linear relationship between the independent factors and the dependent factor (Wang et al., 2004a; Wang et al., 2018; Feng and Hu, 2014). In general, a formula can be written as $y = F(x_1, x_2, x_3, ..., x_n)$ to express the complex connection. Among them, y is the dependent factor and x represents the multiple independent factors. In this study, the future precipitation or temperature is the y variable, GCMs (five levels) and SSPs (two levels) are x variables (Huang et al., 1997; Wang et al., 2021). According to the ANOVA theory, the total variance contains two aspects:

$$SS_{total} = \sum_{i=1}^{n} SS_i + SS_{int} \tag{1}$$

where SS_{total} is the total variance; SS_i represents the variance of a single factor; SS_{int} is expressed as the variance of interactions between multiple factors. The SS_{int} also can be written as:

$$SS_{int} = \sum_{i=1}^{n} \sum_{j>i}^{n} SS_{ij} + ... + SS_{1,2,...,n} = SS_{total} - \sum_{i=1}^{n} SS_i \tag{2}$$

The ratio of the variance of each part to the total variance is regarded as the contribution of the main effect and the interactive effect to the total effect, respectively. The variance fraction p can be calculated as follows:

$$p_i = \frac{SS_i}{SS_{total}} \times 100\% \tag{3}$$

$$p_{int} = \frac{SS_{int}}{SS_{total}} \times 100\% \tag{4}$$

Table 2 presents the detailed multi-factorial design for future precipitation and temperature projection. In this study, two factors (i.e., GCM with five levels and SSP with two levels) and two responses (i.e., precipitation and temperature) are

TABLE 2 | The multi-level factorial design for the sources of uncertainty of future precipitation and temperature projection.

Levels	Factors		Response	
	GCMs (x_1)	SSPs (x_2)	Precipitation	Temperature
1	CESM2	SSP245	y_{1-1}	y_{2-1}
2	CESM2	SSP585	y_{1-2}	y_{2-2}
3	GFDL-ESM4	SSP245	y_{1-3}	y_{2-3}
4	GFDL-ESM4	SSP585	y_{1-4}	y_{2-4}
5	IPSL-CM6A-LR	SSP245	y_{1-5}	y_{2-5}
6	IPSL-CM6A-LR	SSP585	y_{1-6}	y_{2-6}
7	MIROC6	SSP245	y_{1-7}	y_{2-7}
8	MIROC6	SSP585	y_{1-8}	y_{2-8}
9	MRI-ESM2-0	SSP245	y_{1-9}	y_{2-9}
10	MRI-ESM2-0	SSP585	y_{1-10}	y_{2-10}

employed (**Figure 2**). Therefore, there are a total of ten different level combinations in this design.

RESULTS

Spatial-Temporal Trends in Precipitation and Temperature

Figure 3 presents the Mann-Kendall trend analysis results for annual precipitation and annual mean temperature in the historical and future periods. MK trend analysis is a non-parametric test method broadly employed to statistically evaluate whether there is a significant change trend in a time sequence of the corresponding variable. The null hypothesis, H_0, indicates that there is no monotonic trend. The alternative hypothesis, H_1, states that there is a positive or negative monotonic trend in the data series. More details can be found in previous study (Duan et al., 2021). For the annual precipitation, nearly half of the areas (47.8%) show a significant trend in the historical period. Among them, the central areas in China present a significant decreasing trend. In the Northwest China, there is a significant growth trend. The significant proportion reached 70.3%. In the Northeast China and North China, the significant proportions are relatively small, at 4.4 and 7.6%, respectively. The fraction of China areas with a significant trend will be increased to 52.7% during 2051–2100 under SSP245. Besides, the annual precipitation will be increased to varying degrees in all seven sub-regions. The central areas, South China, and Northeast China have a statistically significant (indicate by dots) increasing trend for annual precipitation. The significant proportion of precipitation increase in North China and Northeast China has increased compared with the historical period. The significant proportions in the Northeast China and North China have reached 80.3 and 24.4%, respectively. The percentage of significant trend areas will continually increase to 85.5% during 2051–2100 under SSP585. Meanwhile, there will be a significantly high increase center in Southwest China. The significant proportions in Northwest China and Northeast China exceed 90%. In North China, Central China, Southwest China, and South China, proportions exceed 80%. The trend change in annual mean temperature is in sharp contrast with
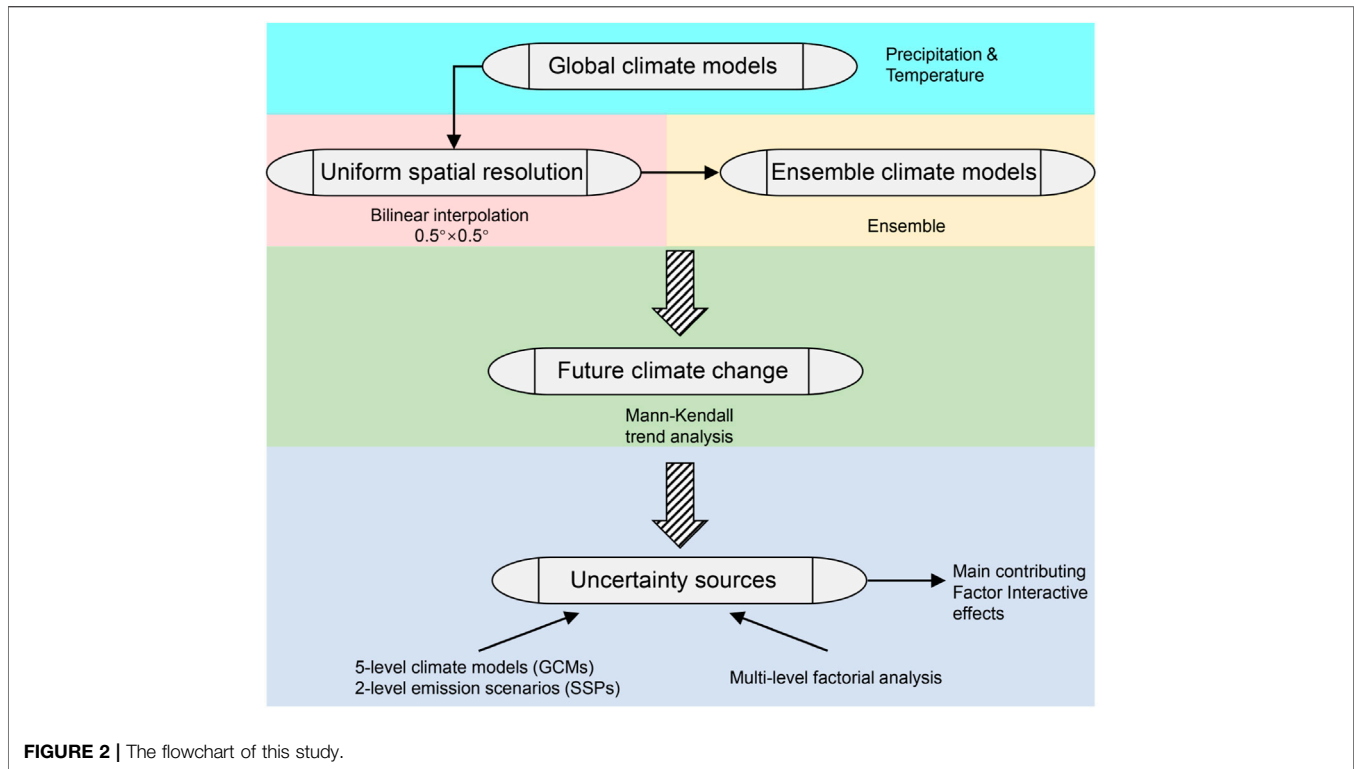
FIGURE 2 | The flowchart of this study.

annual precipitation. It has shown a significant increasing trend both in historical (99.9% significant trend areas) and future periods (100% significant trend areas) over China areas. The growth rate is the largest during 2051–2100 under SSP585, which is 0.1°C/year. In general, over China areas, the annual precipitation and annual mean temperature will increase significantly in the future, especially under SSP585. In historical and future periods, the northwestern inland temperature has increased relatively high. Compared with precipitation, the temperature has increased significantly throughout China, especially in the future. That means China will face higher temperature in the future, and there may be more temperature-related extreme climate events. It is also consistent with previous research conclusions (Chaudhuri et al., 2020; Ramil et al., 2020; Shrestha and Wang, 2020).

Projections of Future Precipitation and Temperature

Figure 4 shows the variations of future annual precipitation and annual mean temperature under SSP245 and SSP585. Compared with the historical period, the annual precipitation will increase by 11.3% over whole China areas, under SSP245. Besides, the precipitation will also increase to varying degrees in the seven sub-regions. Among them, the growth rate of the inland northwest area is higher than that of the northern and eastern coastal regions. In general, the increase in the northern part is higher than that in the southern region. The fraction of entire China areas with increasing annual precipitation will reach to 17.2% under SSP585. The growth rate of the inland northwest

area is still higher than that of the eastern regions. Compared with the historical period, the whole China areas will be much wetter due to the increase annual precipitation. Among them, the proportion of precipitation increase in Northwest China, North China, and Northeast China is about 19%. The southwestern region is 18%, and the rest parts are about 10%. **Figure 4** also presents the change in annual mean temperature. Undoubtedly, temperature will increase in the future, both under SSP245 and SSP585. The increasing annual mean temperature over the whole China areas is 2.8°C under SSP245, and under SSP585, this increment will be 4.7°C. Interestingly, the spatial pattern of annual mean temperature variations is quite similar to precipitation, under both SSPs. Temperature increase in Northeast China, North China, and Northwest China is higher than that in the southern regions. The temperature increase is 3.2, 3.0, and 3.0°C, respectively, under SSP245. While under SSP585, the increase is further expanded to 5.2, 5.0, and 5.0°C, respectively. The temperature increase in the other four sub-regions was relatively small. Under SSP245, the increase is around 2°C, and under SSP585, the increase is around 4°C.

In summary, the results indicate that both annual precipitation and annual mean temperature over China will increase in the future. Regardless of SSP245 or SSP585, the growth rate of annual precipitation and annual mean temperature increase in the northern region (e.g., Northeast China, North China, and Northwest China) are higher than those in the southern parts (e.g., East China, South China, and Central China). The increase in precipitation is closely related to the rise in temperature, and it has been discussed in previous studies. Potential evapotranspiration will be increased with the
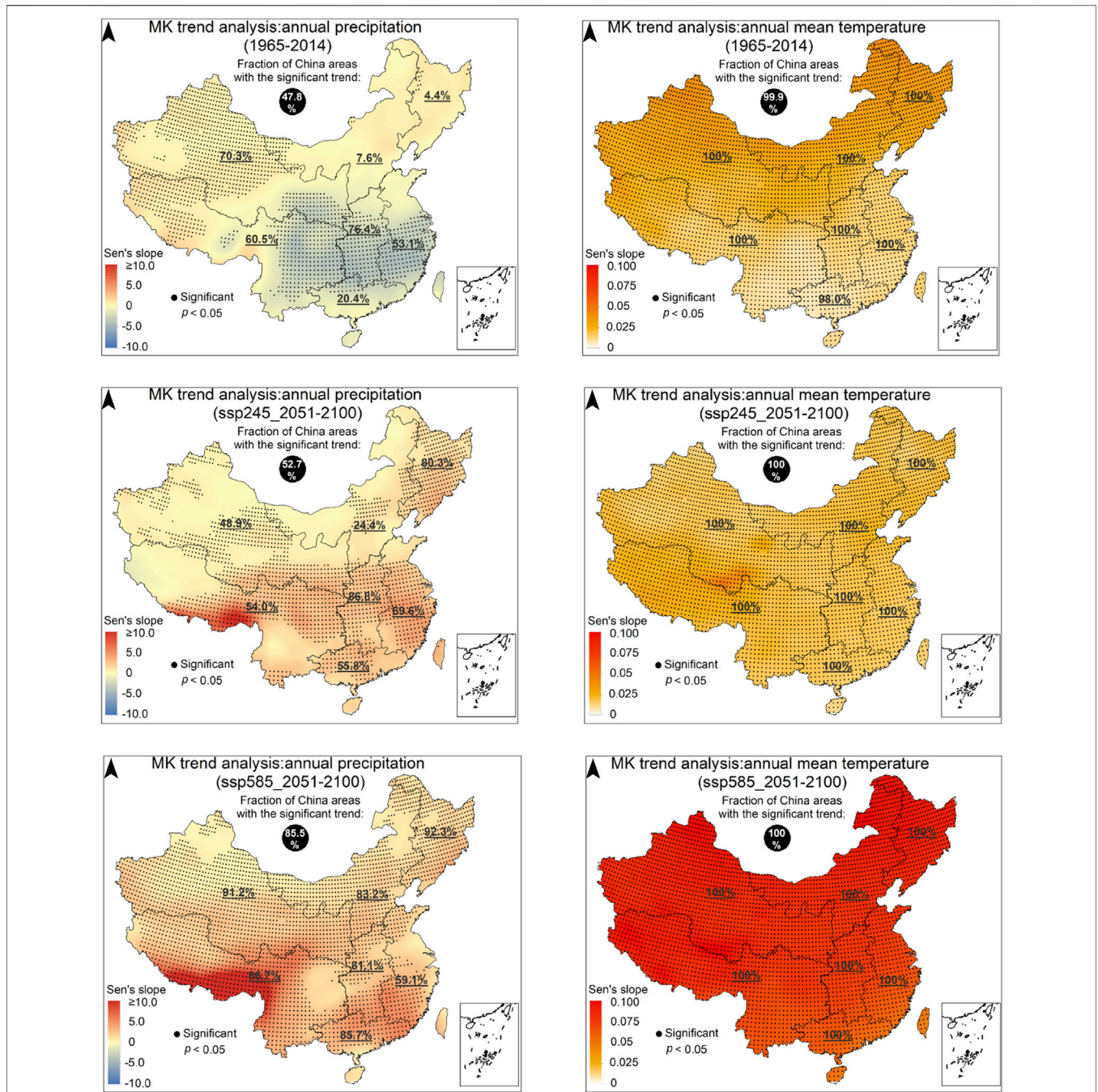
FIGURE 3 | The results of Mann-Kendall trend analysis for annual precipitation and annual mean temperature during the historical and future periods. The historical period is 1965–2014, and the future period is 2051–2100 under SSP245 and SSP585.

rise in temperature, and it may cause large amounts of moisture to converge. Eventually lead to a large increase in precipitation. Changes in precipitation and temperature will affect many aspects of China. Such as the agricultural output, human health, and infrastructure. The future temperature rise may increase the frequency of heat-related extreme climate events, which needs to be focused on in future research.

Figure 5 visually shows the historical and future changes in annual precipitation and annual mean temperature in China and the seven sub-regions. The results provide more detailed statistics
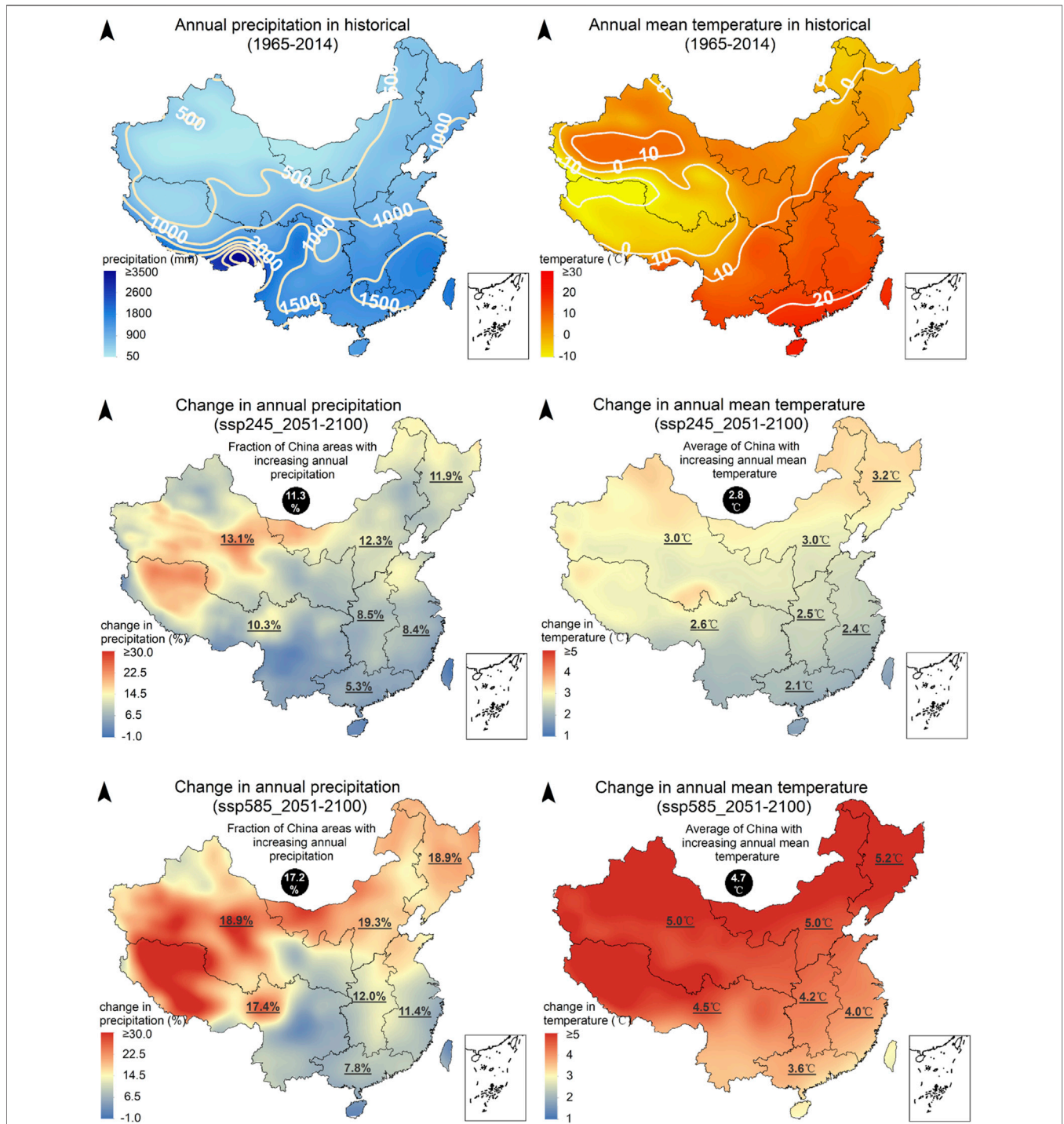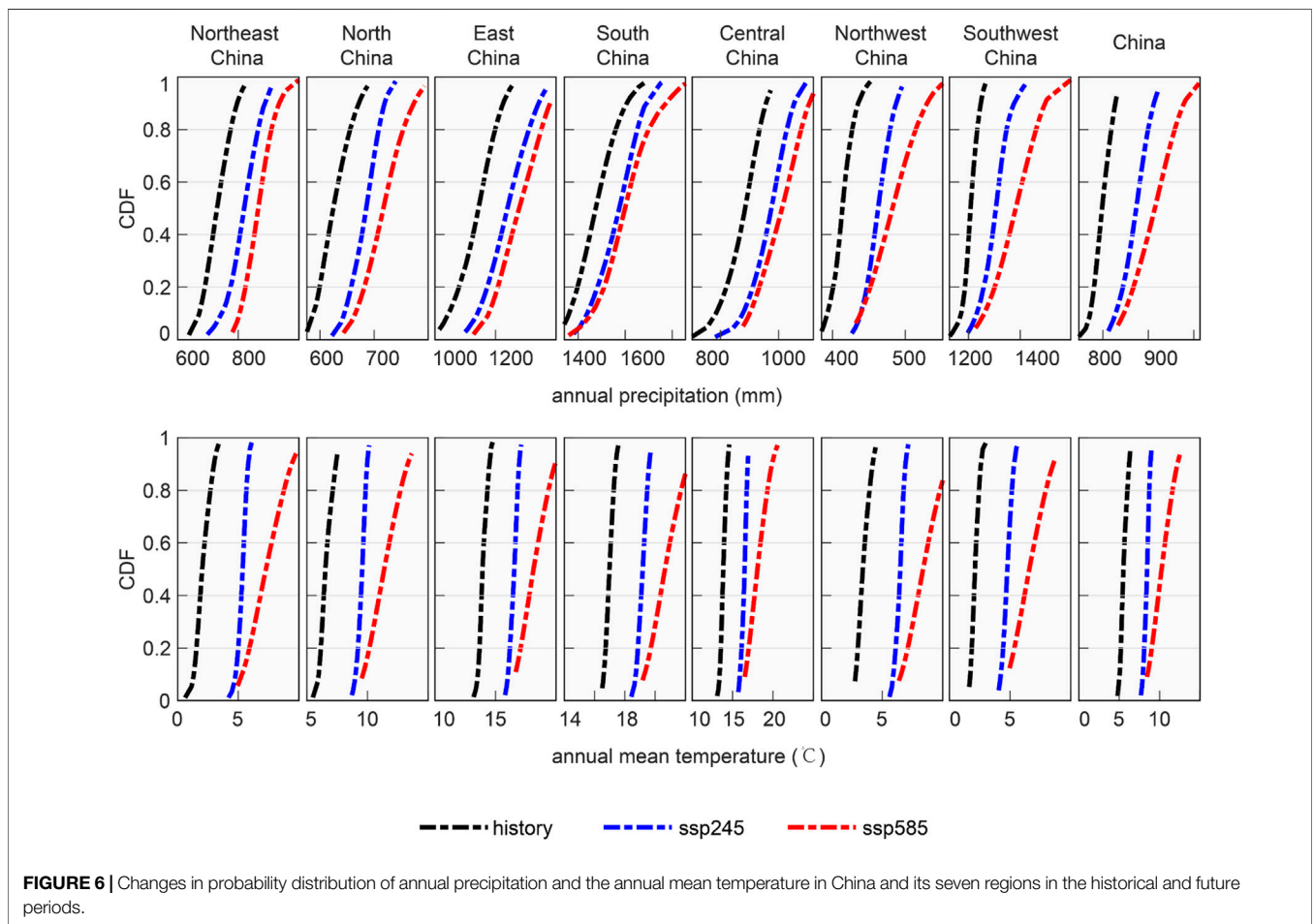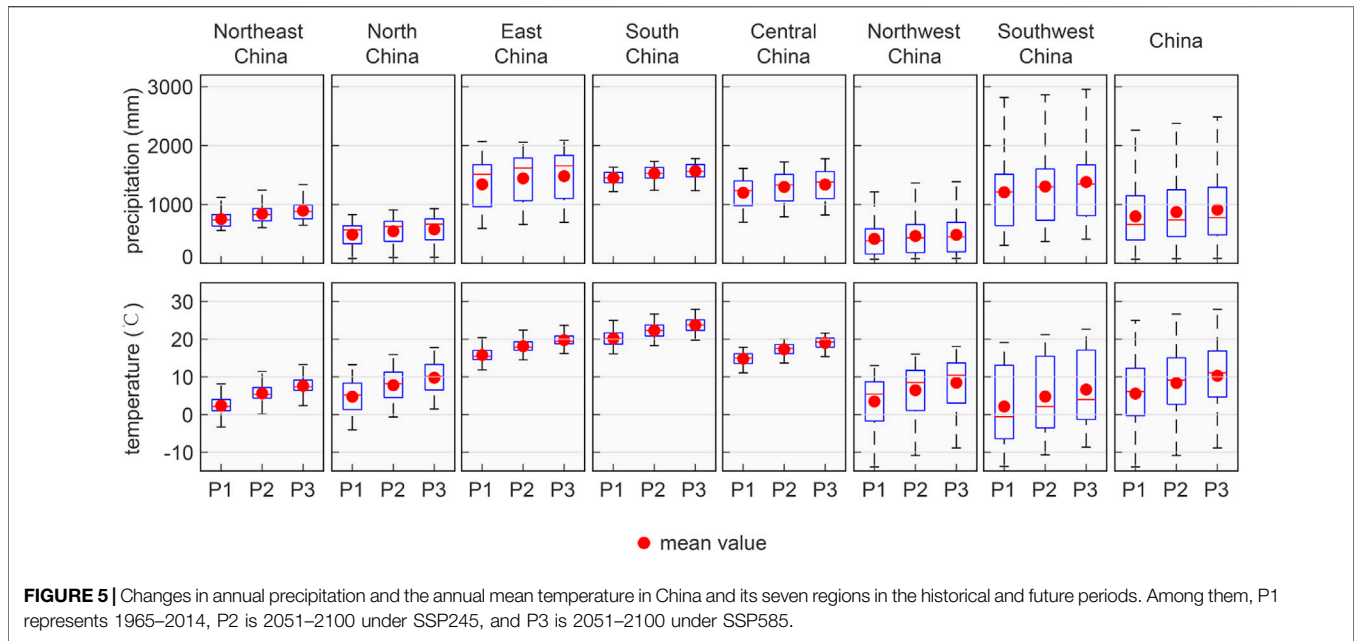
FIGURE 4 | The change in spatial distribution of annual precipitation and annual mean temperature during 2051–2100 under two SSPs relative to the historical period.

on the changes in precipitation and temperature. Precipitation in East China, South China, Central China, and Southwest China is much more. However, the growth rate in the future is significantly lower than that of other regions, as shown in **Figure 4**. The results also indicate that the previously wet areas will be wetter, while the

dry areas tend to be wet. For the annual mean temperature, the East China, South China, and Central China will face higher temperature.

Figure 6 presents the changes in the probability distribution of annual precipitation and annual mean temperature. The black
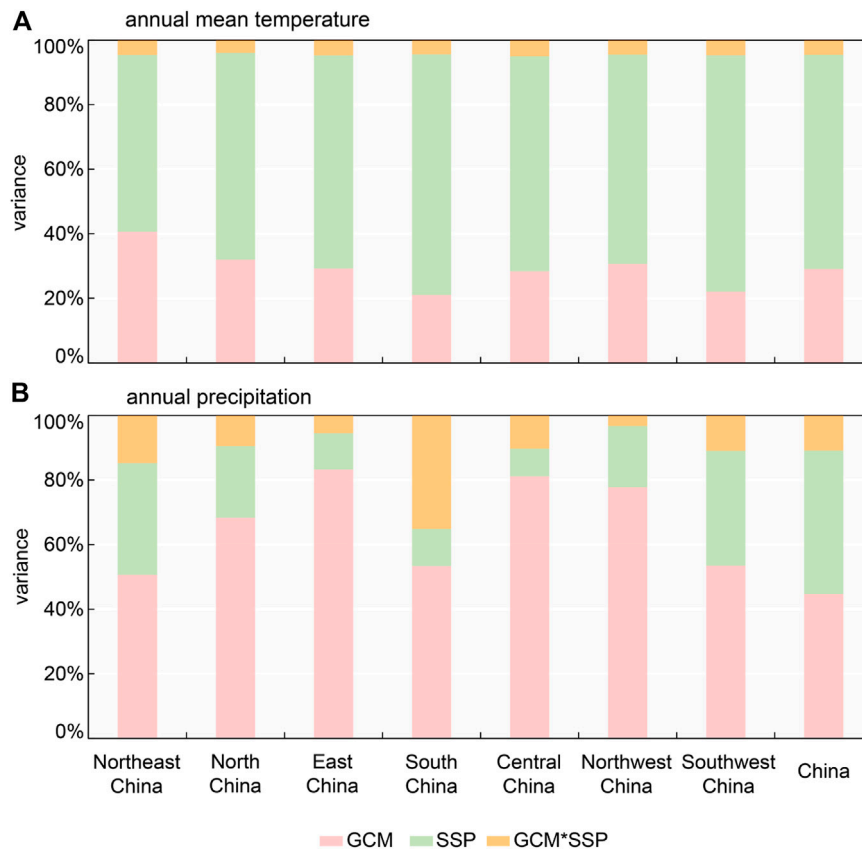
FIGURE 5 | Changes in annual precipitation and the annual mean temperature in China and its seven regions in the historical and future periods. Among them, P1 represents 1965–2014, P2 is 2051–2100 under SSP245, and P3 is 2051–2100 under SSP585.

FIGURE 6 | Changes in probability distribution of annual precipitation and the annual mean temperature in China and its seven regions in the historical and future periods.

FIGURE 7 | The main contribution (and their interactions) of GCM and SSP to the sources of uncertainty on annual precipitation and annual mean temperature projections over China and seven sub-regions.

line represents the distribution of precipitation and temperature in the historical period. The blue line is the probability distribution of the two variables in 2051–2100 under SSP245, and the red line represents the probability variation of the two variables in 2051–2100 under SSP585. Compared with the historical period, the probability distribution of precipitation and temperature under SSP245 and SSP585 both shifted to the right. The results also show that under the SSP scenarios, the seven sub-regions and the entire China area will have more precipitation and higher temperature in the future. Climate change has significant impacts on China, and the regional ecological environment and human production may face severe challenges in the future due to changes in temperature and precipitation, as well as their derivative disasters (e.g., drought). Therefore, a full understanding of the possible impacts of climate change on China is desired.

Contributing Factors to Variations of Precipitation and Temperature

The uncertainties come from various factors, such as GCMs and SSPs. In this study, GCMs (with five levels) and SSPs (with two levels) are employed to quantify the main and interactive effects on precipitation and temperature projection. As presented in

Figure 7, the total variance of precipitation and temperature projection contains three aspects: GCMs, SSPs, and their interactions. For annual precipitation, the largest contributing factor to the total variance comes from GCM, with the rate of 50.68% (Northeast China), 68.33% (North China), 83.28% (East China), 53.35% (South China), 81.20% (Central China), 77.79% (Northwest China), 53.49% (Southwest China), and 44.73% (entire China), respectively. The second contributing factor is SSP, with the rate of 34.63% (Northeast China), 22.25% (North China), 11.17% (East China), 11.52% (South China), 8.50% (Central China), 18.91% (Northwest China), 35.56% (Southwest China), and 44.36% (entire China), respectively. The contribution of the interaction is relatively small, with the rate of 14.69% (Northeast China), 9.42% (North China), 5.54% (East China), 35.13% (South China), 10.30% (Central China), 3.30% (Northwest China), 10.95% (Southwest China), and 10.91% (entire China), respectively.

For annual mean temperature, the largest contributing factor to the total variance comes from SSP, with the rate of 54.75% (Northeast China), 64.08% (North China), 65.96% (East China), 74.60% (South China), 66.66% (Central China), 64.84% (Northwest China), 73.22% (Southwest China), and 66.42% (entire China), respectively. The second contributing factor is GCM, with the rate of 40.64% (Northeast China),32.02% (North

China), 29.25% (East China), 21.04% (South China), 28.42% (Central China), 30.70% (Northwest China), 22.07% (Southwest China), and 29.09% (entire China), respectively. The contribution of the interaction is relatively small, with the rate of 4.61% (Northeast China), 3.91% (North China), 4.80% (East China), 4.35% (South China), 4.92% (Central China), 4.46% (Northwest China), 4.71% (Southwest China), and 4.49% (entire China), respectively.

The projections of future precipitation and temperature have the uncertainty of global climate models and emission scenarios. Results show that GCM is the main source of uncertainties in precipitation projection. For all sub-regions, the main contributing factor to the total variance in precipitation projection is GCM. The average contribution portions are all exceeded 50%. The interaction between GCM and SSP is relatively small. Results also present that SSP is the major contributing factor to the total variance in temperature projection. The average contribution portions are also exceeded 50%. Besides, the interaction between GCM and SSP is also quite small. Different variables have different sources of uncertainty. This may reflect the influence of different parameterization schemes of the model on the final output result.

DISCUSSION

The study on future precipitation and temperature projection, based on ensemble of global climate models, has the uncertainties of different emission scenarios and climate models. The uncertainty of future climate projection may have a profound impact on climate change projection and assessment. It is necessary to quantify different sources of uncertainty to provide reliable output achieve (Tisseuil et al., 2012; Feng and Hu, 2014). The relationship between the independent variables (i.e., climate models and emission scenarios) and the response variable is not a simple linear relationship. It is hard to explore their main and interactive effects on response variables. Nevertheless, the application of factorial analysis can roughly explore the main effects and interactions of various factors behind complex nonlinear relationships. Therefore, GCMs with five levels and SSPs with two levels are employed to trace the sources of uncertainty in projecting future precipitation and temperature, and the multi-factorial analysis method is used in this study. Results show that the major contributing factors in projecting future precipitation are all GCM over seven sub-regions and entire China. However, the major contributing factors in projecting future temperature are all SSP over seven sub-regions and entire China (Chen et al., 2016; Manrique-Alba et al., 2020). The effects explained by GCM and SSP interactions are relatively small for both future precipitation and temperature projection. To trace the different sources of uncertainty in projecting future climate change, multiple qualitative and quantitative methods have been employed in previous studies, such as the ANOVA theory.

The different kinds of uncertainties sources of multiple climate models perhaps lie in the insufficient cognizing and understanding on the natural earth change process of global climate change. Ultimately, the outputs of climate models accompany various assumptions and limitations. Due to the unpredictability of social-economic factor and human behavior in the future period, a variety of potential greenhouse gas emission scenarios have been generated (Shivam et al., 2019; Sharafi et al., 2020). For instance, the Representative Concentration Pathways (RCPs) in CMIP5 and the Shared Socioeconomic Pathways (SSPs) in CMIP6. Different emission scenarios have multiple premises and assumptions, which represent variations of development paths in the future (Du et al., 2018). Although developers try to incorporate the main physical processes of the earth's natural changes into the climate model, due to unknown emission scenarios, imperfect model structure, and complex climate systems, the simulation output of the climate model is bound to be uncertain. To reduce the system uncertainty in the modeling process as much as possible, the calculation and simulation are usually carried out through ensemble means of multiple GCMs (Moore et al., 2013; Smalley et al., 2019). A variety of ensemble methods have been developed in previous studies. In this study, five different GCMs under two SSPs are given equal weights. After the ensemble process, future annual precipitation and annual mean temperature are then projected. The simulation performance of multiple GCMs will vary with different variables and the study area. Besides, due to some GCMs share the same parameterization scheme, some modules or codes, different GCMs are not completely independent (Vogel et al., 2020; Zhai et al., 2020). Therefore, in this study, giving the same weight to all GCMs may not be the optimal solution to achieve ensemble. Wang et al. (2019) have assessed eight different weighting schemes to determine the optimal weight distribution among multiple GCMs. In addition, the effects of different weighting schemes on the final output simulation results are also compared (Wang et al., 2019). The performance of multiple GCMs ensemble has been confirmed in many studies, and the ability to project future climate change is better than a single GCM. Perhaps the multiple GCMs ensemble can reduce the systematic bias from the individual GCM, thereby improving the ability to project future variables. In the current climate change-related study, GCM is the only tool that can be used, but due to its shortcomings, the projection of some climate variables has a large deviation. In future research, reducing the systemic bias of the climate model itself will undoubtedly be the top priority (Chen et al., 2016; Wang et al., 2018).

CONCLUSION

In this study, future annual precipitation and annual mean temperature under two SSPs over China areas were projected through multiple global climate models. Meanwhile, to explore the sources of uncertainty in projecting future climate change, the multi-factorial analysis was conducted through GCMs (five levels) and SSPs (two levels). This study can help us understand the possible changes in precipitation, temperature, and the potential extreme climate events over the China area. The results indicate that China would have more annual precipitation

and higher annual mean temperature in the future. Compared with the historical period, the annual mean temperature would face a continuously increasing trend under SSPs. Regardless of SSP245 or SSP585, the growth rate of annual precipitation and annual mean temperature increase in the northern region (e.g., Northeast China, North China, and Northwest China) are higher than those in the southern parts (e.g., East China, South China, and Central China). The increase in precipitation is closely related to the rise in temperature. Potential evapotranspiration would be increased with the temperature rise, and it could cause large amounts of moisture to converge. Eventually, this leads to a large increase in precipitation. Changes in precipitation and temperature would affect many aspects of China. Such as the agricultural output, human health, and infrastructure. The future temperature rise may increase the frequency of heat-related extreme climate events, which needs to be focused on in future research. Moreover, GCM was the main contributing factor to the source of uncertainty in projecting future precipitation and SSP was the main factor for future temperature. The interactive effects are relatively unobvious on both projecting precipitation and temperature.

Overall, climate change is an indisputable fact in China. The annual precipitation and annual mean temperature will increase to varying degrees in the future. Reducing the systemic bias of the climate model itself will undoubtedly be the top priority, and it will help improve the projection and evaluation effects of relevant climate variables.

DATA AVAILABILITY STATEMENT

The original contributions presented in the study are included in the article/Supplementary Material, further inquiries can be directed to the corresponding author.

AUTHOR CONTRIBUTIONS

FUNDING

REFERENCES

Asif, Z., Chen, Z., and Chen, Z. (2020). A Life Cycle Based Air Quality Modeling and Decision Support System (LCAQMS) for Sustainable Mining Management. *J. Environ. Inform.* 35 (2), 103–117. doi:10.3808/jei.201900406

Ba, W., Du, P., Liu, T., Bao, A., Luo, M., Hassan, M., et al. (2018). Simulating Hydrological Responses to Climate Change Using Dynamic and Statistical Downscaling Methods: a Case Study in the Kaidu River Basin, Xinjiang, China. *J. Arid Land.* 10, 905–920. doi:10.1007/s40333-018-0068-0

Batibeniz, F., Ashfaq, M., Diffenbaugh, N. S., Key, K., Evans, K. J., Turuncoglu, U. U., et al. (2020). Doubling of U.S. Population Exposure to Climate Extremes by 2050. *Earth's Future* 8. doi:10.1029/2019EF001421

Carrão, H., Naumann, G., and Barbosa, P. (2016). Mapping Global Patterns of Drought Risk: An Empirical Framework Based on Sub-national Estimates of hazard, Exposure and Vulnerability. *Glob. Environ. Change.* 39, 108–124. doi:10.1016/j.gloenvcha.2016.04.012

Chaudhuri, S., Roy, M., Roy, M., and Jain, A. (2020). Appraisal of Wash (Water-sanitation-hygiene) Infrastructure Using a Composite index, Spatial Algorithms and Sociodemographic Correlates in Rural India. *J. Env Inform.* 35 (1), 1–22. doi:10.3808/jei.201800398

Chen, Y. D., Li, J., and Zhang, Q. (2016). Changes in Site-Scale Temperature Extremes over China during 2071-2100 in CMIP5 Simulations. *J. Geophys. Res. Atmos.* 121, 2732–2749. doi:10.1002/2015JD024287

Cheng, T. F., Lu, M., and Dai, L. (2019). The Zonal Oscillation and the Driving Mechanisms of the Extreme Western North Pacific Subtropical High and its Impacts on East Asian Summer Precipitation. *J. Clim.* 32, 3025–3050. doi:10.1175/JCLI-D-18-0076.1

Cho, M.-H., Boo, K.-O., Martin, G. M., Lee, J., and Lim, G.-H. (2015). The Impact of Land Cover Generated by a Dynamic Vegetation Model on Climate over East Asia in Present and Possible Future Climate. *Earth Syst. Dynam.* 6, 147–160. doi:10.5194/esd-6-147-2015

Dan, L., Cao, F., and Gao, R. (2015). The Improvement of a Regional Climate Model by Coupling a Land Surface Model with Eco-Physiological Processes: A Case Study in 1998. *Climatic Change.* 129, 457–470. doi:10.1007/s10584-013-0997-8

Du, L., Mikle, N., Zou, Z., Huang, Y., Shi, Z., Jiang, L., et al. (2018). Global Patterns of Extreme Drought-Induced Loss in Land Primary Production: Identifying Ecological Extremes from Rain-Use Efficiency. *Sci. Total Environ.* 628-629, 611–620. doi:10.1016/j.scitotenv.2018.02.114

Duan, R., Huang, G., Li, Y., Zhou, X., Ren, J., and Tian, C. (2021). Stepwise Clustering Future Meteorological Drought Projection and Multi-Level Factorial Analysis under Climate Change: A Case Study of the Pearl River Basin, China. *Environ. Res.* 196, 110368. doi:10.1016/j.envres.2020.110368

Duan, R., Huang, G., Zhou, X., Li, Y., and Tian, C. (2021). Ensemble Drought Exposure Projection for Multifactorial Interactive Effects of Climate Change and Population Dynamics: Application to the Pearl River Basin. *Earth's Future.* 9, e2021EF002215. doi:10.1029/2021EF002215

Feng, J., and Hu, D. (2014). How Much Does Heat Content of the Western Tropical Pacific Ocean Modulate the South China Sea Summer Monsoon Onset in the Last Four Decades? *J. Geophys. Res. Oceans.* 119, 4029–4044. doi:10.1002/2013JC009683

Ghosh, S., and Mujumdar, P. P. (2007). Nonparametric Methods for Modeling GCM and Scenario Uncertainty in Drought Assessment. *Water Resour. Res.* 43. doi:10.1029/2006WR005351

Hou, Y.-k., He, Y.-f., Chen, H., Xu, C.-Y., Chen, J., Kim, J.-S., et al. (2019). Comparison of Multiple Downscaling Techniques for Climate Change Projections Given the Different Climatic Zones in China. *Theor. Appl. Climatol.* 138, 27–45. doi:10.1007/s00704-019-02794-z

Huang, G. H., Baetz, B. W., Patry, G. G., and Terluk, V. (1997). Capacity Planning for an Integrated Waste Management System under Uncertainty: a North American Case Study. *Waste Manag. Res.* 15, 523–546. doi:10.1177/0734242x9701500507

Hui, P., Tang, J., Wang, S., Niu, X., Zong, P., and Dong, X. (2018). Climate Change Projections over China Using Regional Climate Models Forced by Two CMIP5 Global Models. Part II: Projections of Future Climate. *Int. J. Climatol.* 38, e78–e94. doi:10.1002/joc.5409

Jacob, D., Kotova, L., Teichmann, C., Sobolowski, S. P., Vautard, R., Donnelly, C., et al. (2018). Climate Impacts in Europe under +1.5°C Global Warming. *Earth's Future.* 6, 264–285. doi:10.1002/2017EF000710

Ji, D., Dong, W., Hong, T., Dai, T., Zheng, Z., Yang, S., et al. (2018). Assessing Parameter Importance of the Weather Research and Forecasting Model Based

on Global Sensitivity Analysis Methods. *J. Geophys. Res. Atmos.* 123, 4443–4460. doi:10.1002/2017JD027348

Kodinariya, T. M., and Makwana, P. R. (2013). Review on Determining Number of Cluster in K-Means Clustering. *Int. J. Adv. Res. Comput. Sci. Manag. Stud.* 1 (6), 90–95.

Li, L., Lei, L., Lei, L., Zheng, M. S., Borthwick, A. G. L., and Ni, J. R. (2020). Stochastic Evolutionary-Based Optimization for Rapid Diagnosis and Energy-Saving in Pilot- and Full-Scale Carrousel Oxidation Ditches. *J. Env Inform.* 35 (1), 81–93. doi:10.3808/jei.201700377

Li, Y. F., Li, Y. P., Huang, G. H., and Chen, X. (2010). Energy and Environmental Systems Planning under Uncertainty-An Inexact Fuzzy-Stochastic Programming Approach. *Appl. Energ.* 87, 3189–3211. doi:10.1016/j.apenergy.2010.02.030

Manrique-Alba, À., Beguería, S., Molina, A. J., González-Sanchis, M., Tomàs-Burguera, M., del Campo, A. D., et al. (2020). Long-term Thinning Effects on Tree Growth, Drought Response and Water Use Efficiency at Two Aleppo pine Plantations in Spain. *Sci. Total Environ.* 728, 138536. doi:10.1016/j.scitotenv.2020.138536

Moore, J. K., Lindsay, K., Doney, S. C., Long, M. C., and Misumi, K. (2013). Marine Ecosystem Dynamics and Biogeochemical Cycling in the Community Earth System Model [CESM1(BGC)]: Comparison of the 1990s with the 2090s under the RCP4.5 and RCP8.5 Scenarios. *J. Clim.* 26, 9291–9312. doi:10.1175/JCLI-D-12-00566.1

Paeth, H., and Hense, A. (2004). SST versus Climate Change Signals in West African Rainfall: 20th-century Variations and Future Projections. *Climatic Change.* 65, 179–208. doi:10.1023/B:CLIM.0000037508.88115.8a

Park, C., Min, S.-K., Lee, D., Cha, D.-H., Suh, M.-S., Kang, H.-S., et al. (2016). Evaluation of Multiple Regional Climate Models for Summer Climate Extremes over East Asia. *Clim. Dyn.* 46, 2469–2486. doi:10.1007/s00382-015-2713-z

Peltier, W. R., d'Orgeville, M., Erler, A. R., and Xie, F. (2018). Uncertainty in Future Summer Precipitation in the Laurentian Great Lakes basin: Dynamical Downscaling and the Influence of continental-scale Processes on Regional Climate Change. *J. Clim.* 31, 2651–2673. doi:10.1175/JCLI-D-17-0416.1

Poschlod, B., Hodnebrog, Ø., Wood, R. R., Alterskjær, K., Ludwig, R., Myhre, G., et al. (2018). Comparison and Evaluation of Statistical Rainfall Disaggregation and High-Resolution Dynamical Downscaling over Complex Terrain. *J. Hydrometeorol.* 19, 1973–1982. doi:10.1175/JHM-D-18-0132.1

Ramil, A., Vázquez-Nion, D., Vázquez-Nion, D., Pozo-Antonio, J. S., Sanmartín, P., and Prieto, B. (2020). Using Hyperspectral Imaging to Quantify Phototrophic Biofilms on Granite. *J. Env Inform* 35 (1), 34–44. doi:10.3808/jei.201800401

Roberts, J. L., Tozer, C. R., Ho, M., Kiem, A. S., Vance, T. R., Jong, L. M., et al. (2019). Reconciling Unevenly Sampled Paleoclimate Proxies: A Gaussian Kernel Correlation Multiproxy Reconstruction. *J. Environ. Inform* 35 (2), 1–10. doi:10.3808/jei.201900420

Sharafi, L., Zarafshani, K., Keshavarz, M., Azadi, H., and Van Passel, S. (2020). Drought Risk Assessment: Towards Drought Early Warning System and Sustainable Environment in Western Iran. *Ecol. Indicators.* 114, 106276. doi:10.1016/j.ecolind.2020.106276

Shivam, G., Goyal, M. K., Goyal, M. K., and Sarma, A. K. (2019). Index-based Study of Future Precipitation Changes over Subansiri River Catchment under Changing Climate. *J. Env Inform.* 34 (1), 1–14. doi:10.3808/jei.201700376

Shrestha, N. K., Wang, J., and Wang, J. (2020). Water Quality Management of a Cold Climate Region Watershed in Changing Climate. *J. Environ. Inform* 35 (1), 56–80. doi:10.3808/jei.201900407

Smalley, K. M., Glisan, J. M., and Gutowski, W. J. (2019). Alaska Daily Extreme Precipitation Processes in a Subset of CMIP5 Global Climate Models. *J. Geophys. Res. Atmos.* 124, 4584–4600. doi:10.1029/2018JD028643

Smirnov, O., Zhang, M., Xiao, T., Orbell, J., Lobben, A., and Gordon, J. (2016). The Relative Importance of Climate Change and Population Growth for Exposure to Future Extreme Droughts. *Climatic Change.* 138, 41–53. doi:10.1007/s10584-016-1716-z

Spinoni, J., Barbosa, P., Bucchignani, E., Cassano, J., Cavazos, T., Christensen, J. H., et al. (2020). Future Global Meteorological Drought Hot Spots: A Study Based on CORDEX Data. *J. Clim.* 33, 3635–3661. doi:10.1175/jcli-d-19-0084.1

Tan, Q., Huang, G. H., and Cai, Y. P. (2011). Radial Interval Chance-Constrained Programming for Agricultural Non-point Source Water Pollution Control under Uncertainty. *Agric. Water Manage.* 98, 1595–1606. doi:10.1016/j.agwat.2011.05.013

Thomas, D. S. K., Wilhelmi, O. V., Finnessey, T. N., and Deheza, V. (2013). A Comprehensive Framework for Tourism and Recreation Drought Vulnerability Reduction. *Environ. Res. Lett.* 8, 044004. doi:10.1088/1748-9326/8/4/044004

Thompson, G., Tewari, M., Ikeda, K., Tessendorf, S., Weeks, C., Otkin, J., et al. (2016). Explicitly-coupled Cloud Physics and Radiation Parameterizations and Subsequent Evaluation in WRF High-Resolution Convective Forecasts. *Atmos. Res.* 168, 92–104. doi:10.1016/j.atmosres.2015.09.005

Tisseuil, C., Vrac, M., Grenouillet, G., Wade, A. J., Gevrey, M., Oberdorff, T., et al. (2012). Strengthening the Link between Climate, Hydrological and Species Distribution Modeling to Assess the Impacts of Climate Change on Freshwater Biodiversity. *Sci. Total Environ.* 424, 193–201. doi:10.1016/j.scitotenv.2012.02.035

Trenberth, K. E., and Shea, D. J. (2005). Relationships between Precipitation and Surface Temperature. *Geophys. Res. Lett.* 32. doi:10.1029/2005GL022760

Vogel, M. M., Hauser, M., and Seneviratne, S. I. (2020). Projected Changes in Hot, Dry and Wet Extreme Events' Clusters in CMIP6 Multi-Model Ensemble. *Environ. Res. Lett.* 15, 094021. doi:10.1088/1748-9326/ab90a7

Wang, B., LinHoZhang, Y., and Lu, M. M. (2004a). Definition of South China Sea Monsoon Onset and Commencement of the East Asia Summer Monsoon*. *J. Clim.* 17, 699–710. doi:10.1175/2932.1

Wang, F., Huang, G. H., Fan, Y., and Li, Y. P. (2021). Development of Clustered Polynomial Chaos Expansion Model for Stochastic Hydrological Prediction. *J. Hydrol.* 595, 126022. doi:10.1016/j.jhydrol.2021.126022

Wang, H.-M., Chen, J., Xu, C.-Y., Chen, H., Guo, S., Xie, P., et al. (2019). Does the Weighting of Climate Simulations Result in a Better Quantification of Hydrological Impacts? *Hydrol. Earth Syst. Sci.* 23, 4033–4050. doi:10.5194/hess-23-4033-2019

Wang, Y., Leung, L. R., McGregor, J. L., Lee, D.-K., Wang, W.-C., Ding, Y., et al. (2004b). Regional Climate Modeling: Progress, Challenges, and Prospects. *J. Meteorol. Soc. Jpn.* 82, 1599–1628. doi:10.2151/jmsj.82.1599

Wang, Z., Zhong, R., Lai, C., Zeng, Z., Lian, Y., and Bai, X. (2018). Climate Change Enhances the Severity and Variability of Drought in the Pearl River Basin in South China in the 21st century. *Agric. For. Meteorology* 249, 149–162. doi:10.1016/j.agrformet.2017.12.077

Ying, J., Huang, P., and Lian, T. (2019). Changes in the Sensitivity of Tropical Rainfall Response to Local Sea Surface Temperature Anomalies under Global Warming. *Int. J. Climatol.* 39, 5801–5814. doi:10.1002/joc.6303

Zhai, A. F., Ding, X. W., Ding, X. W., Zhao, Y., Xiao, W. H., and Lu, B. X. (2020). Improvement of Instantaneous point Source Model for Simulating Radionuclide Diffusion in Oceans under Nuclear Power Plant Accidents. *J. Environ. Inform* 36 (2), 133–145. doi:10.3808/jei.201700380

Zhou, X., Huang, G., Wang, X., and Cheng, G. (2018). Dynamically-downscaled Temperature and Precipitation Changes over Saskatchewan Using the PRECIS Model. *Clim. Dyn.* 50, 1321–1334. doi:10.1007/s00382-017-3687-9